

A DVS-MHE Approach to Vehicle Side-Slip Angle Estimation

M. Canale*, L. Fagiano[†], C. Novara*

Abstract—A study on the application of a Moving Horizon Estimator (MHE) to the problem of vehicle side-slip angle estimation is carried out. In particular, it is shown that a stable MHE can be represented as Nonlinear Finite Impulse Response (NFIR) filter. Then, in order to allow online implementation and guaranteed estimation accuracy, an optimal NFIR filter is derived directly from data by means of a Direct Virtual Sensor (DVS) approach. Comparisons between the standard model based MHE approach and the DVS one are carried using a detailed vehicle model.

I. INTRODUCTION

Significant improvements on safety and handling performance have been obtained through active control systems recently introduced on production vehicles (see e.g. [1],[2],[3]). Such systems are based on suitable control strategies which use the measure of variables related to lateral vehicle dynamics. The most common solution is the use of a yaw rate feedback, since its measure can be realized by means of quite cheap sensors.

As a matter of fact, in emergency braking or turning maneuvers it is needed to avoid too large values of the side-slip angle β in order to enhance vehicle safety (see [4]). Besides, the side-slip angle has to be limited to low values (e.g. $\pm 4^\circ$) to improve the stability feelings perceived by the driver. Therefore, performance improvements can be achieved if a side-slip angle feedback is employed too. On the other hand, an accurate measure of the side-slip angle can be only obtained through complex and expensive sensors not available on commercial cars. A viable solution to this problem is to use the information coming from other already mounted sensors (e.g. gyro, accelerometer, ...) in order to provide an estimate of β through an observer. Indeed, side-slip angle observer design is a well known and challenging topic and several solutions appeared in recent years. In particular, linear and nonlinear approaches have been proposed on the basis of well assessed estimation frameworks such as Extended Kalman filters, Luenberger and sliding mode observers (see e.g. [5], [6] and [7]). In order to design such observers, physical, possibly nonlinear, models of the vehicle are used. However, these models depend on physical parameters which are unknown or difficult to estimate. Yet, the side-slip angle depends on the driving conditions (e.g. speed, road friction,

...) which may change during vehicle maneuvers. In order to circumvent such problems, adaptive estimation approaches have been recently introduced in [8] and [9], and the use of identified Linear Parameter Varying (LPV) models has been successfully investigated in [10] and [11].

Another point that has to be highlighted is that the side-slip angle observers are usually obtained according to a two steps procedure. In the first step, a vehicle model is derived using experimental data. In the second step, the observer is designed on the basis of such a model. However, as shown in [12], this procedure is in general not optimal, since models derived from data are approximate and estimators designed from such models may display a performance degradation when applied to the real system. An innovative approach was introduced in [13], where the use of the Direct Virtual Sensor (DVS) methodology has been employed for side-slip angle estimation, avoiding the use of whatever physical or identified model in the observer design. In the DVS approach, the observer is obtained directly from the data collected under different driving conditions. General theoretical results about DVSSs can be found in [14], [12] and [15], together with a number of experimental and simulation results.

In this paper, a solution based on a Moving Horizon Estimation (MHE) approach (see [16], [17]), which has been already employed in the context of side-slip angle estimation (see [18]), will be considered. MHE filters have interesting features, like the possibility to guarantee the filter stability in the presence of nonlinear dynamics and to handle constraints on the variables to be estimated. However, it has to be noted that this methodology suffers the problem of online implementation, since it involves the solution of a nonlinear program at each sampling time. Furthermore, the usual framework of MHE requires the knowledge of a model of the system, with the already mentioned problems related to model identification and modeling errors. These problems may be circumvented by adopting the DVS technique, using data measured on the vehicle to directly design the filter. It will be shown that the MHE algorithm implicitly defines a Nonlinear Finite Impulse Response (NFIR) filter, which depends on present and past values of the available system (i.e. the vehicle) measurements. On the basis of this consideration, several DVSSs with NFIR structure will be designed and compared with the MHE filters, to evaluate their respective advantages and drawbacks in the problem of side-slip angle estimation.

The paper is organized as follows. The problem of the side-slip angle estimation is introduced in Section II. The MHE approach is described in Section III, while the proposed solution obtained through the use of DVS is presented in Section IV. In Section V, the MHE and the DVS side-slip

* Dipartimento di Automatica e Informatica, Politecnico di Torino, Italy. [†] ABB Switzerland Ltd, Switzerland.

Email addresses: massimo.canale@polito.it, lorenzo.fagiano@ch.abb.com, carlo.novara@polito.it.

A preliminary version of this paper has been included in the Proceedings of the 49th IEEE Conference on Decision and Control, Atlanta (GA), USA, 2010.

estimators are designed and their performance are compared through simulations performed using a detailed vehicle model. Concluding remarks end the paper.

II. ESTIMATION OF VEHICLE SIDE-SLIP ANGLE

The lateral vehicle dynamics can be described through the following nonlinear single track vehicle model (see e.g. [2]):

$$\begin{aligned}
M\dot{a}_y(t) &= F_{yf}(t) + F_{yr}(t) + Mw_2(t) \\
J_z\dot{\psi}(t) &= aF_{yf}(t) - bF_{yr}(t) + w_1(t) \\
F_{yf}(t) + l_f/v_x(t)\dot{F}_{yf}(t) &= F_{yf}^P(\alpha_{wf}) \\
F_{yr}(t) + l_r/v_x(t)\dot{F}_{yr}(t) &= F_{yr}^P(\alpha_{wr}) \\
a_y(t) &= \dot{v}_y(t) + v_x(t)\dot{\psi}(t) \\
\alpha_{wf}(t) &= -\beta(t) - a\dot{\psi}(t)/v_x(t) + \delta_D(t)/\tau_D \\
\alpha_{wr}(t) &= -\beta(t) + b\dot{\psi}(t)/v_x(t)
\end{aligned} \tag{1}$$

where δ_D is the handwheel angle, commanded by the driver, a_y is the lateral acceleration and v_x and v_y are the vehicle longitudinal and lateral speeds, respectively. Moreover, M is the vehicle mass, J_z is the moment of inertia around the vertical axis, β is the side-slip angle, ψ is the yaw angle, a and b are the distances between the center of gravity and the front and rear axles respectively, while l_f and l_r are the front and rear tire relaxation lengths. τ_D is the transmission ratio between the handwheel angle and the steering angles of the front wheels (which are assumed to be the same for the left and right wheels), $w_1(t)$ and $w_2(t)$ are external disturbances accounting for yaw moments and lateral forces respectively, e.g. due to lateral wind acting on the vehicle. Finally, F_{yf} and F_{yr} are the front and rear tire lateral forces, which can be expressed as nonlinear functions of the wheel front and rear side-slip angles, α_{wf} and α_{wr} respectively, by using the renown ‘‘magic formula’’ (see [19] and [20] for more details):

$$\begin{aligned}
F_{yf}^P(\alpha_{wf}) &= D_{wf}(C_{wf} \arctan(B_{wf}(\alpha_{wf}) \\
&\quad - E_{wf}(B_{wf}(\alpha_{wf}) - \arctan(B_{wf}(\alpha_{wf})))) \\
F_{yr}^P(\alpha_{wr}) &= D_{wr}(C_{wr} \arctan(B_{wr}(\alpha_{wr}) \\
&\quad - E_{wr}(B_{wr}(\alpha_{wr}) - \arctan(B_{wr}(\alpha_{wr}))))
\end{aligned} \tag{2}$$

where B_{wf} , C_{wf} , D_{wf} , E_{wf} , B_{wr} , C_{wr} , D_{wr} , E_{wr} are parameters which can be identified, for a given vehicle, through standard maneuvers like steering pads.

In vehicle active control systems, the variables involved in the lateral dynamics description such as the longitudinal speed v_x , the lateral acceleration a_y , the yaw rate $\dot{\psi}$ and the side-slip angle β can be employed by a feedback controller in order to compute the control input for suitable actuation devices, such as active differentials, active braking systems and active front/rear steering systems (see e.g. [21] and the references therein). However, while measurements or estimates of v_x , $\dot{\psi}$ and a_y can be obtained using cheap sensors like wheel speed sensors, gyroscopes and accelerometers, side-slip angle sensors are much more expensive and, as a consequence, the vehicle side-slip angle is usually not employed in active stability control. Yet, the angle β is strongly related to vehicle directional stability and its use in feedback control together with the other variables could bring forth significant performance improvements [21].

In this paper, the aim is to derive an algorithm to estimate the vehicle side-slip angle β using other available measurements. In particular, two different approaches are considered and compared. In the first one, described in Section III, a Moving Horizon Estimation framework is considered, in which the filter is derived on the basis of the model (1), by solving online a suitable optimization problem. The second approach, treated in Section IV, relies on the direct design of the filter from measured data.

III. MOVING HORIZON ESTIMATION

Consider a discrete-time nonlinear system described in state-space form:

$$\begin{aligned}
x^{t+1} &= F(x^t, \tilde{u}^t, w^t) \\
\tilde{y}^t &= H_y(x^t, \tilde{u}^t, w^t) \\
v^t &= H_v(x^t, \tilde{u}^t)
\end{aligned} \tag{3}$$

where $t \in \mathbb{N}$, $x^t \in \mathbb{R}^{n_x}$ is the system state, $\tilde{u}^t \in \mathbb{R}^{n_u}$ is the known input, $\tilde{y}^t \in \mathbb{R}^{n_y}$ is a measured output, $w^t \in \mathbb{R}^{n_w}$ is an unmeasured disturbance, and $v^t \in \mathbb{R}^{n_v}$ is an unmeasured variable of interest. Note that in (3) w^t is a vector that includes both process and measurement disturbances.

In the following, a sequence of input values starting from time step t_1 up to time step t_2 will be denoted by $\tilde{U}_{t_1}^{t_2} = \{\tilde{u}^t\}_{t=t_1}^{t_2}$. Likewise, $\tilde{Y}_{t_1}^{t_2}$ and $W_{t_1}^{t_2}$ denote sequences of outputs and disturbances. The predicted trajectory of the state of system (3) at time step t obtained by starting from the state x^{t-j} at time step $t-j$ and by applying given sequences of inputs \tilde{U}_{t-j}^{t-1} and disturbances W_{t-j}^{t-1} is indicated as $x(t, t-j, x^{t-j}, \tilde{U}_{t-j}^{t-1}, W_{t-j}^{t-1})$, while the disturbance-free predicted trajectory (i.e. $W_{t-j}^{t-1} = 0$) is denoted by $x(t, t-j, x^{t-j}, \tilde{U}_{t-j}^{t-1})$. Similar notations are used to denote the predicted output y and the predicted unmeasured variable v at time t .

It is assumed that, at any step t , the disturbance w^t and the variable v^t belong to the compact sets $\mathcal{W} \in \mathbb{R}^{n_w}$ and $\mathcal{V} \in \mathbb{R}^{n_v}$ respectively. The sets \mathcal{W} and \mathcal{V} are usually chosen on the basis of the available physical insight of the system. Finally, the system (3) is assumed to be uniformly observable, according to the following definition (see e.g. [22]).

Definition 1: A system of the form (3) is uniformly observable if, for any two state values x_1^t and x_2^t , there exist a finite number of time steps N_o and a \mathcal{K} -function ζ such that, for any given sequence of inputs $\tilde{U}_t^{\overline{t}+N_o-1}$:

$$\zeta(\|x_1^t - x_2^t\|) \leq \sum_{j=0}^{N_o-1} \|y(t+j, t, x_1^t, \tilde{U}_t^{\overline{t}+j}) - y(t+j, t, x_2^t, \tilde{U}_t^{\overline{t}+j})\|. \blacksquare$$

We recall that a continuous real function $\zeta(z)$ is a \mathcal{K} -function if it is strictly monotone increasing, $\zeta(0) = 0$, $\zeta(z) > 0$ for any $z \neq 0$ and $\lim_{z \rightarrow \infty} \zeta(z) = \infty$. In such a framework, the problem considered in this work can be stated as follows:

Problem 1: Find a function f (‘‘estimation algorithm’’, ‘‘estimator’’ or ‘‘filter’’) that, operating on \tilde{u}^τ and \tilde{y}^τ , $\tau \leq t$, computes, at each time step t , an estimate $\hat{v}^t \approx v^t$ such that $\hat{v}^t \in \mathcal{V}$, whose estimation error $e^t = v^t - \hat{v}^t$ is bounded in

some norm and possibly minimal with respect to a suitable optimization criterion. ■

Obviously, if $v^t = x^t$, the described problem is equivalent to a state estimation problem, but, in general, one could be interested in estimating also other system variables. Due to the presence of constraints on the variable v , it is not easy to solve Problem 1 even in the case of a linear system (i.e. when functions F , H_y and H_v in (3) are linear). Moreover, the presence of nonlinearities further increases the difficulty of Problem 1. Most of the design techniques employed in the literature to address Problem 1 rely on the knowledge of the system equations (3), of an initial estimate \bar{x}^{t-j} of the system state at a suitably chosen time step $t-j$ and of sequences of past measured output and input values, $\tilde{Y}_{t-\tau}^t$ and $\tilde{U}_{t-\tau}^t$ respectively, up to a finite number $\tau+1$ of past time steps. Among such techniques, Moving Horizon Estimation (MHE) is widely recognized as one of the most promising due to its capability to take into account explicitly the system nonlinearities and constraints. In MHE, a cost function of the following form is considered:

$$\begin{aligned} & J(\hat{x}^{t-\tau}, \tilde{U}_{t-\tau}^t, W_{t-\tau}^t, \tilde{Y}_{t-\tau}^t, \bar{x}^{t-\tau}) \\ &= \sum_{j=0}^{\tau} L(e_y^{t-\tau+j}, w^{t-\tau+j}) + \Phi(\bar{x}^{t-\tau}, \hat{x}^{t-\tau}), \end{aligned} \quad (4)$$

where the output error $e_y^{t-\tau+j}$, $j=0, \dots, \tau$ is defined as

$$e_y^{t-\tau+j} = \tilde{y}^{t-\tau+j} - y(t-\tau+j, t-\tau, \hat{x}^{t-\tau}, \tilde{U}_{t-\tau}^{t-\tau+j}, W_{t-\tau}^{t-\tau+j}). \quad (5)$$

In (4) the initial state guess $\bar{x}^{t-\tau}$ and the sequences $\tilde{Y}_{t-\tau}^t$, $\tilde{U}_{t-\tau}^t$ of measured outputs and inputs are known parameters in the optimization, while the initial state estimate $\hat{x}^{t-\tau}$ and the disturbance sequence $W_{t-\tau}^t$ are optimization variables and the length $N = \tau + 1$ of $\tilde{U}_{t-\tau}^t$ and of $\tilde{Y}_{t-\tau}^t$ is a design parameter, as well as the stage cost function $L(\cdot, \cdot)$ and the initial cost function $\Phi(\cdot, \cdot)$. Then, Problem 1 is cast in a numerical optimization framework, in which the following minimization problem has to be solved:

$$\min_{\hat{x}^{t-\tau}, W_{t-\tau}^t} J(\hat{x}^{t-\tau}, \tilde{U}_{t-\tau}^t, W_{t-\tau}^t, \tilde{Y}_{t-\tau}^t, \bar{x}^{t-\tau}) \quad (6a)$$

subject to

$$v(t-\tau+j, t-\tau, \hat{x}^{t-\tau}, \tilde{U}_{t-\tau}^{t-\tau+j}, W_{t-\tau}^{t-\tau+j}) \in \mathcal{V}, \quad \forall j \in [0, \tau] \quad (6b)$$

$$w(t-\tau+j) \in \mathcal{W}, \quad \forall j \in [0, \tau]. \quad (6c)$$

If a solution $(\hat{x}^{t-\tau*}, W_{t-\tau}^{t*})$ to (6) is found, the estimate \hat{v}^{MHE} is computed as the predicted value of v starting from the optimized initial state guess $\hat{x}^{t-\tau*}$ and applying the optimal sequence $W_{t-\tau}^{t*}$ and the measured sequence $\tilde{U}_{t-\tau}^t$:

$$\hat{v}^{\text{MHE}} = v(t, t-\tau, \hat{x}^{t-\tau*}, \tilde{U}_{t-\tau}^t, W_{t-\tau}^{t*}). \quad (7)$$

Finally, problem (6) is solved at each time step after having updated the sequences $\tilde{Y}_{t-\tau}^t$ and $\tilde{U}_{t-\tau}^t$ with new measurements, according to the following Moving Horizon strategy:

- 1) At time step t , update the sequences $\tilde{Y}_{t-\tau}^t$ and $\tilde{U}_{t-\tau}^t$ with the measured variables \tilde{y}^t , \tilde{u}^t ;

- 2) update the initial state guess as $\bar{x}^{t-\tau} = x(t-\tau, t-\tau-1, \hat{x}^{t-\tau-1*}, \tilde{U}_{t-\tau-1}^{t-\tau}, W_{t-\tau-1}^{t-\tau*})$, where $W_{t-\tau-1}^{t-\tau*}$ is part of the the optimal disturbance sequence $W_{t-\tau-1}^{t-1*}$, computed at time step $t-1$, and $\hat{x}^{t-\tau-1*}$ is the optimal initial state computed at time step $t-1$;
- 3) solve the optimization problem (6) to compute $\hat{x}^{t-\tau*}$ and $W_{t-\tau}^{t*}$;
- 4) compute the estimate \hat{v}^{MHE} (7);
- 5) repeat the procedure from step 1) at time step $t+1$.

Although MHE is a powerful approach whose diffusion is increasing, some critical problems are still open. One of these issues is the possible non-convexity of the nonlinear program (6). Finding the global minimum of (6) may be extremely hard, whereas local minima of this function, which are more easy to be found, may lead to poor estimates and/or “jumps” in the estimated variable between two subsequent time steps. A second relevant drawback is that, in many practical applications, the online implementation of a MHE can not be performed, since the minimization problem (6) may not be solved for small sampling times. Finally, another problem, shared by the MHE approach with all the other model-based design methods (e.g. the Extended Kalman Filter), is that the system (3) in most practical situations is not (exactly) known. Thus, in order to design a model-based estimation algorithm a two-step procedure is usually adopted: 1) a model of the system is identified from data; 2) the estimation algorithm is designed on the basis of the identified model. In general, the two-step procedure is not optimal and does not allow the evaluation of guaranteed accuracy performance of the filter in terms e.g. of bounds of the estimation error [12].

A new approach to estimator design is now introduced, which may be used to overcome these problems. The approach is based on the fact that, once the design parameters N , $L(\cdot, \cdot)$ and $\Phi(\cdot, \cdot)$ have been chosen, the MHE procedure implicitly defines an estimation algorithm f^{MHE} whose arguments are the initial state guess $\bar{x}^{t-\tau}$ and the measured sequences $\tilde{Y}_{t-\tau}^t$ and $\tilde{U}_{t-\tau}^t$:

$$\hat{v}^{\text{MHE}} = f^{\text{MHE}}(\tilde{Y}_{t-\tau}^t, \tilde{U}_{t-\tau}^t, \bar{x}^{t-\tau}). \quad (8)$$

Moreover, from step 2) of the MHE strategy it can be noted that, at each time step t , the initial state guess $\bar{x}^{t-\tau}$ is a function of the sequences $\tilde{Y}_{t-\tau-1}^{t-1}$ and $\tilde{U}_{t-\tau-1}^{t-1}$ and of the initial state guess $\bar{x}^{t-\tau-1}$, i.e.

$$\bar{x}^{t-\tau} = g(\tilde{Y}_{t-\tau-1}^{t-1}, \tilde{U}_{t-\tau-1}^{t-1}, \bar{x}^{t-\tau-1}).$$

Then, the estimate (8) can be also expressed, with a slight abuse of notation, as

$$\hat{v}^{\text{MHE}} = f^{\text{MHE}}(\tilde{Y}_{t-\tau-1}^t, \tilde{U}_{t-\tau-1}^t, \bar{x}^{t-\tau-1}), \quad (9)$$

where

$$\begin{aligned} & f^{\text{MHE}}(\tilde{Y}_{t-\tau-1}^t, \tilde{U}_{t-\tau-1}^t, \bar{x}^{t-\tau-1}) \\ &= f^{\text{MHE}}(\tilde{Y}_{t-\tau}^t, \tilde{U}_{t-\tau}^t, g(\tilde{Y}_{t-\tau-1}^{t-1}, \tilde{U}_{t-\tau-1}^{t-1}, \bar{x}^{t-\tau-1})). \end{aligned}$$

Thus, assuming that the MHE algorithm (8) is set up at time step $t_0 + \tau$ with an initial state guess \bar{x}^{t_0} , the estimate \hat{v}^{MHE} at the generic time t can be also expressed as

$$\hat{v}^{\text{MHE}} = f^{\text{MHE}}(\tilde{Y}_{t_0}^t, \tilde{U}_{t_0}^t, \bar{x}^{t_0}), \quad (10)$$

where, again with a slight abuse of notation, f^{MHE} is the function given by the recursive application of (9). A quite wide literature exists (see e.g. [17], [22] and the references therein) regarding the study of sufficient conditions on the system (3), on the constraint sets \mathcal{V}, \mathcal{W} and on the design parameters $N, L(\cdot, \cdot), \Phi(\cdot, \cdot)$ so that the estimator is asymptotically stable. The notion of asymptotic stability considered in the present paper is similar to the one in [22] and can be introduced as follows.

Definition 2: An estimator f^{MHE} is asymptotically stable if, for any arbitrarily small $\epsilon > 0$, there exists a sufficiently large number of time steps m such that, for any initial time t_0 , any $t \geq t_0 + m$, any $\tilde{U}_{t_0}^t$ and $\tilde{Y}_{t_0}^t$, and any two initial state guesses $\tilde{x}_1^{t_0}$ and $\tilde{x}_2^{t_0}$, it holds that $\|f^{\text{MHE}}(\tilde{Y}_{t_0}^t, \tilde{U}_{t_0}^t, \tilde{x}_1^{t_0}) - f^{\text{MHE}}(\tilde{Y}_{t_0}^t, \tilde{U}_{t_0}^t, \tilde{x}_2^{t_0})\| \leq \epsilon$. ■

According to this definition, the effect of the ‘‘initial condition’’ (the initial state guess \tilde{x}^{t_0}) on the estimate of a stable estimator fades away. Thus, after a suitable (possibly large) number m of time steps it can be considered that the estimate \hat{v}^{t_0+m} depends only on the sequences $\tilde{Y}_{t_0}^{t_0+m}, \tilde{U}_{t_0}^{t_0+m}$ and not on the initial state guess \tilde{x}^{t_0} . The following proposition formalizes this concept, showing that a stable MHE estimation algorithm can be expressed as a Nonlinear Finite Impulse Response (NFIR) estimator f_o^{MHE} plus a ‘‘small’’ truncation error e_{trunc}^t .

Proposition 1: Assume that f^{MHE} is asymptotically stable. Then, for any $\epsilon > 0$ and any \tilde{x}^{t_0} , there exist a sufficiently large $m \geq \tau$ and a function f_o^{MHE} such that

$$f^{\text{MHE}}(\tilde{Y}_{t_0}^t, \tilde{U}_{t_0}^t, \tilde{x}^{t_0}) = f_o^{\text{MHE}}(\tilde{Y}_{t_0}^t, \tilde{U}_{t_0}^t) + e_{trunc}^t \quad (11)$$

where $|e_{trunc}^t| \leq \epsilon, \forall t \geq t_0 + m$.

Proof. Let us consider that $t = t_0 + m$ and explicit the dependence on m of f^{MHE} by defining $f_m^{\text{MHE}}(\tilde{Y}_{t_0}^{t_0+m}, \tilde{U}_{t_0}^{t_0+m}, \tilde{x}^{t_0}) \doteq f^{\text{MHE}}(\tilde{Y}_{t_0}^t, \tilde{U}_{t_0}^t, \tilde{x}^{t_0})$. Then,

$$\begin{aligned} f_m^{\text{MHE}}(\tilde{Y}_{t_0}^t, \tilde{U}_{t_0}^t, \tilde{x}^{t_0}) &= f_{t-t_0}^{\text{MHE}}(\tilde{Y}_{t_0}^t, \tilde{U}_{t_0}^t, \tilde{x}^{t_0}) \\ &= f_m^{\text{MHE}}(\tilde{Y}_{t-m}^t, \tilde{U}_{t-m}^t, \tilde{x}^{t-m}). \end{aligned}$$

Since by assumption f^{MHE} is asymptotically stable, for any $\epsilon > 0$, a sufficiently large $m \geq \tau$ exists such that

$$\|f_m^{\text{MHE}}(\tilde{Y}_{t-m}^t, \tilde{U}_{t-m}^t, \tilde{x}^{t-m}) - f_m^{\text{MHE}}(\tilde{Y}_{t-m}^t, \tilde{U}_{t-m}^t, 0)\| \leq \epsilon$$

for any initial time $t - m$, any $\tilde{U}_{t-m}^t \in \mathbb{R}^{n_u \times (m+1)}$ and $\tilde{Y}_{t-m}^t \in \mathbb{R}^{n_y \times (m+1)}$, and any initial state guess $\tilde{x}^{t-m} \in \mathbb{R}^{n_x}$.

The claim follows taking $f_o^{\text{MHE}}(\tilde{Y}_{t-m}^t, \tilde{U}_{t-m}^t) = f_{t-m}^{\text{MHE}}(\tilde{Y}_{t-m}^t, \tilde{U}_{t-m}^t, 0)$. ■

Note that, in general, both f^{MHE} and f_o^{MHE} are ‘‘ideal’’ and not known, due to the above-mentioned issues of non-convexity of problem (6) and modelling errors. Based on Proposition 1, the approach proposed in this paper is to identify, directly from a set of data generated by the system (3), a NFIR estimator approximating f_o^{MHE} , which enjoys suitable optimality properties. The identified estimator is called Direct Virtual Sensor (DVS). The following problem is thus considered in the next Section:

Problem 2: Given a set of data

$$D = \{\tilde{u}^t, \tilde{y}^t, \tilde{v}^t\}_{t=1}^T \quad (12)$$

where $\tilde{v}^t \doteq v^t + \xi^t$ is the measured value of v^t corrupted by the noise ξ^t , find a DVS with estimation error minimal with respect to a suitable criterion. ■

IV. DESIGN OF OPTIMAL DIRECT VIRTUAL SENSORS

In this Section, an approach is presented for the direct design from data of optimal DVSSs. The case $v^t \in \mathbb{R}$ and $\mathcal{V} = [\underline{v}, \bar{v}]$ is considered for simplicity of notation. Variables of higher dimensions can be treated by considering each component as a separate scalar to be estimated.

The aim is to find a NFIR estimator

$$\hat{v}^t = \hat{f}(\tilde{\varphi}_{t-m}^t), \quad \tilde{\varphi}_{t-m}^t \doteq (\tilde{Y}_{t-m}^t, \tilde{U}_{t-m}^t) \quad (13)$$

with estimation error $v^t - \hat{v}^t = v^t - \hat{f}(\tilde{\varphi}_{t-m}^t)$ minimal with respect to a suitable criterion.

The estimator \hat{f} is selected within the following set of Lipschitz continuous functions

$$\begin{aligned} \mathcal{F}(\gamma, m) &\doteq \{f : |f(\varphi_{t-m}^t) - f(\hat{\varphi}_{t-m}^t)| \\ &\leq \gamma \|\varphi_{t-m}^t - \hat{\varphi}_{t-m}^t\|_\infty, \forall \varphi_{t-m}^t, \hat{\varphi}_{t-m}^t \in \Phi\} \end{aligned} \quad (14)$$

where $\|\cdot\|_\infty$ is the ℓ_∞ norm, γ is the Lipschitz constant and Φ is the regressor domain which is assumed to be a bounded convex subset of $\mathbb{R}^{(m+1)(n_y+n_u)}$. The motivation for considering this set are (a) to obtain an estimator with suitable regularity properties; (b) to ensure optimality properties for the designed estimator (see Theorem 1 below). Results on the estimation of constrained Lipschitz continuous functions can be found in [25].

Let us define the estimator f_o as the best approximation within the set $\mathcal{F}(\gamma, m)$ of the MHE estimator f_o^{MHE} in (11):

$$f_o \doteq \arg \min_{f \in \mathcal{F}(\gamma, m)} \|f_o^{\text{MHE}} - f\|_\infty \quad (15)$$

where $\|f\|_\infty \doteq \text{ess sup}_{\varphi \in \Phi} |f(\varphi)|$ is the L_∞ functional norm. Note that, if the MHE optimization problem (6) is convex in both the optimization variables and the parameters, as it happens e.g. when the optimization problem (6) is either a linear or a quadratic program, then $f_o^{\text{MHE}} \in \mathcal{F}(\gamma, m)$ (see e.g. [23]) and, consequently, $f_o = f_o^{\text{MHE}}$.

Consider now that the estimation error of an estimator \hat{f} of the form (13) is bounded as

$$\begin{aligned} |v^t - \hat{f}(\tilde{\varphi}_{t-m}^t)| &= |e_o^t + f_o(\tilde{\varphi}_{t-m}^t) - \hat{f}(\tilde{\varphi}_{t-m}^t)| \\ &\leq |e_o^t| + |f_o(\tilde{\varphi}_{t-m}^t) - \hat{f}(\tilde{\varphi}_{t-m}^t)| \end{aligned} \quad (16)$$

where $e_o^t \doteq v^t - f_o(\tilde{\varphi}_{t-m}^t)$ is the estimation error of f_o and $|f_o(\tilde{\varphi}_{t-m}^t) - \hat{f}(\tilde{\varphi}_{t-m}^t)|$ is the bias between the estimator \hat{f} and f_o . Since e_o does not depend on \hat{f} , the aim is to find an estimator \hat{f} giving ‘‘small’’ bias.

Clearly, this bias is not known, since f_o is not known. In order to derive a tight bound on it, some assumptions on e_o^t and $\xi^t \doteq \tilde{v}^t - v^t$ (the measurement error on v^t , see Problem 2) are required. Here, e_o^t is assumed to be bounded as

$$|e_o^t| \leq \delta_o, \quad \forall t$$

for some $\delta_o \geq 0$. Note that, being $f_o \in \mathcal{F}(\gamma, m)$, this assumption is satisfied if the MHE (10) is asymptotically stable. Assuming that ξ^t is also bounded, we have that the noise $d^t \doteq \tilde{v}^t - f_o(\tilde{\varphi}_{t-m}^t) = \xi^t + e_o^t$ is bounded as

$$|d^t| \leq \varepsilon, \quad \forall t$$

for some $\varepsilon \geq 0$. The values of the bound ε on noise and the Lipschitz constant γ can be suitably chosen by means of the validation procedure described in [24]. The value of δ_o is not required for the design of the optimal DVS presented in the following.

On the basis of the above assumptions, the Feasible Estimator Set is now defined.

Definition 3: Feasible Estimator Set:

$$FES \doteq \left\{ f \in \mathcal{F}(m, \gamma) : \left| \tilde{v}^k - f(\tilde{\varphi}_{k-m}^k) \right| \leq \varepsilon, k \in [1, T] \right\}. \quad \blacksquare$$

According to this definition, FES is the smallest set guaranteed to contain f_o . The tightest bound on the bias in (16) is thus given by $\sup_{f \in FES} \left| f(\tilde{\varphi}_{t-m}^t) - \hat{f}(\tilde{\varphi}_{t-m}^t) \right|$, leading to the following definition of worst-case estimation error.

Definition 4: Worst-case estimation error of a DVS \hat{f} :

$$ED(\hat{f}, t) \doteq \delta_o + \sup_{f \in FES} \left| f(\tilde{\varphi}_{t-m}^t) - \hat{f}(\tilde{\varphi}_{t-m}^t) \right|. \quad \blacksquare \quad (17)$$

Looking for a DVS that minimizes this error, we can introduce the following optimality concept.

Definition 5: A DVS f^* is optimal if

$$ED(f^*, t) = \inf_f ED(f, t), \quad \forall t > T. \quad \blacksquare$$

Let us now define the DVS

$$\hat{v}^t = f_c(\tilde{\varphi}_{t-m}^t), \quad t > T \quad (18)$$

where

$$f_c(\varphi) \doteq \frac{1}{2} [\bar{f}(\varphi) + \underline{f}(\varphi)] \quad (19)$$

$$\bar{f}(\varphi) \doteq \min_{k \in [1, T]} \left(\bar{v}, \tilde{v}^k + \varepsilon + \gamma \left\| \varphi - \tilde{\varphi}_{k-m}^k \right\|_{\infty} \right) \quad (20)$$

$$\underline{f}(\varphi) \doteq \max_{k \in [1, T]} \left(\underline{v}, \tilde{v}^k - \varepsilon - \gamma \left\| \varphi - \tilde{\varphi}_{k-m}^k \right\|_{\infty} \right).$$

The following result shows that the DVS (18) is optimal.

Theorem 1:

- (i) The DVS f_c is optimal.
- (ii) The following tight inequalities on v^t holds:

$$\underline{f}(\tilde{\varphi}_{t-m}^t) - \delta_o \leq v^t \leq \bar{f}(\tilde{\varphi}_{t-m}^t) + \delta_o, \quad t > T.$$

- (iii) The worst-case estimation error of f_c is given by

$$ED(f_c, t) = \delta_o + \frac{1}{2} \left[\bar{f}(\tilde{\varphi}_{t-m}^t) - \underline{f}(\tilde{\varphi}_{t-m}^t) \right], \quad t > T. \quad (21)$$

Proof. The proof of claims (i) and (iii) can be obtained by minor modifications of the proof of Theorem 1 in [26]. In this latter proof, it is also shown that $\bar{f}(\tilde{\varphi}_{t-m}^t)$ and $\underline{f}(\tilde{\varphi}_{t-m}^t)$ are the tightest upper and lower bounds of $f_o(\tilde{\varphi}_{t-m}^t)$. Claim

- (ii) thus follows from the fact that $v^t - f_o(\tilde{\varphi}_{t-m}^t) \doteq e_o^t$ and $|e_o^t| \leq \delta_o, \forall t$. \blacksquare

A DVS is essentially a causal and stable dynamic system taking as inputs the input \tilde{u}^t and output \tilde{y}^t of the system whose variable v^t has to be estimated, and giving as output an estimate \hat{v}^t of this variable.

The DVS design procedure can be summarized as follows:

- 1) Collect a set of experimental data from the system whose variable has to be estimated. These data should be sufficiently rich, in the sense that they should be collected under different experimental conditions during maneuvers of different types (a method for assessing the information level of a data set is presented in [27]).
- 2) Choose the order m of the DVS. This choice can be made by means of a trial and error procedure.
- 3) From the collected data, estimate the noise bound ε and the Lipschitz constant γ by means of the validation method in [24].

Once these operations have been completed, the optimal DVS estimator is univocally defined by (18), (19) and (20). The DVS works on a real-time unit as follows. First, the data $\{\tilde{\varphi}_{k-m}^k, \tilde{v}^k\}_{k=1}^T$ and the parameters ε and γ have to be stored in the unit memory. Then, at each time step $t > T$, the function \bar{f} is evaluated for a given $\tilde{\varphi}_{t-m}^t$ through the following steps:

- 1) The quantities $\tilde{v}^k + \varepsilon + \gamma \left\| \tilde{\varphi}_{t-m}^t - \tilde{\varphi}_{k-m}^k \right\|_{\infty}, k \in [1, T]$ are computed.
- 2) $\bar{f}(\tilde{\varphi}_{t-m}^t)$ is obtained by taking the minimum among these T quantities.

The function \underline{f} is evaluated similarly. Note that all these computations require only elementary operations such as sum, multiplication, square roots, minimum and maximum.

Remark 1: Suppose that in (21), $\frac{1}{2} [\bar{f}(\tilde{\varphi}_{t-m}^t) - \underline{f}(\tilde{\varphi}_{t-m}^t)] \ll \delta_o$ for all t . This condition is met if a sufficiently informative data set D is available (a method for assessing the degree of information of a given data set is proposed in [27]). In this case, we have that $ED(f_c, t) \cong \delta_o$, and $f_c \cong f_o$: in other words, the designed DVS has a performance close to the one of the filter that, within the considered class (14), best approximates the ideal MHE filter f_o^{MHE} .

Remark 2: Any Lipschitz continuous function can be optimally approximated by a function f_c of the form (19), see [24], [25]. This important property is used by the DVS approach to approximate the optimal estimator f_o defined in (15). In Section V below, it is shown how this allows us to accurately estimate the complex nonlinear behavior of the vehicle side-slip angle.

V. ESTIMATION OF VEHICLE SIDE-SLIP ANGLE

A. Detailed nonlinear vehicle model

A detailed 14 degrees of freedom (d.o.f.) nonlinear model which provides an accurate description of the vehicle behavior (see [19] and [21] for details) has been used to generate the data required to design the DVS and to test the performance achieved by both the DVS and the MHE filters. The parameters of the model have been identified from experimental data measured on a real car. The model degrees of freedom correspond

to the standard three chassis translations and yaw, pitch and roll angles, the four wheel angular speeds and the four wheel vertical movements with respect to the chassis. Nonlinear characteristics obtained on the basis of measurements on the real vehicle have been employed to model the tire, steer and suspension behavior. The employed tire model takes into account the interaction between longitudinal and lateral slip, as well as vertical tire load and suspension motion, to compute the tire longitudinal and lateral forces and self-aligning moments. Unsymmetrical friction ellipses for traction/braking longitudinal forces are also considered in the model.

The following list shows the matching between the main physical variables involved in the side-slip angle estimation problem and the generic variables employed in Sections III–IV:

- the handwheel angle and the longitudinal speed are the known inputs: $\tilde{u}^t = [\delta_D^t; v_x^t]$; the measures of δ_D^t and v_x^t are corrupted by uniform noises of amplitudes 1° and 1 km/h, respectively;
- the lateral acceleration is the measured output: $\tilde{y}^t = a_y^t$; the measure of this signal is corrupted by a uniform noise of amplitude 0.2 m/s²;
- the side-slip angle is the variable to estimate: $v^t = \beta^t$; the noise ξ^t on side-slip angle measurements $\tilde{v}^t = v^t + \xi^t$ has been simulated as a white noise with standard deviation 0.12° ;
- the disturbance is given by $w^t = [w_1^t; w_2^t]$, where w_1^t and w_2^t correspond to the disturbances $w_1(t)$ and $w_2(t)$ appearing in 1; these two disturbances have been simulated as white Gaussian noises with zero mean and 5% standard deviation ($\text{std}(w_1^t) = 0.05\text{std}(a_y^t)$ and $\text{std}(w_2^t) = 0.05\text{std}(J_z \ddot{\psi}^t)$).

B. MHE design

The nonlinear single track vehicle model (1) has been discretized with sampling time $T_s = 0.01$ s and using Euler approximation, to be used in the MHE filter design. The following values of the model parameters have been used: $M = 1715$ kg, $J_z = 2697$ kgm², $a = 1.07$ m, $b = 1.47$ m, $l_f = 0.1$ m, $l_r = 0.1$ m, $\tau_D = 15.4$, $B_{wf} = 7.822$, $C_{wf} = 1.3$, $D_{wf} = 8824.51$, $E_{wf} = -0.2977$, $B_{wr} = 13.051$, $C_{wr} = 1.3$, $D_{wr} = 6725.16$, $E_{wr} = -0.1594$. Note that these values have been identified from experimental data measured on a real car (the same data used for the identification of the 14 d.o.f. model parameters).

In order to limit the computational complexity, the sequence $W_{t-\tau}^t$ in (6) has been chosen as $W_{t-\tau}^t = 0$ (i.e. zero estimated noise), thus reducing to 4 the number of optimization variables (i.e. the system state at time instant $t - \tau$, see (6)). A zero initial state guess has been used. The cost function (4) has been defined by choosing $L(e) = Q e^2$, with $Q = 1$, and $\Phi(\hat{x}^{t-\tau}, \hat{x}^{t-\tau}) = R (\hat{x}^{t-\tau} - \hat{x}^{t-\tau})^2$, with $R = 0.1$. The chosen values of Q and R have been tuned through numerical simulations with the detailed nonlinear vehicle model, in order to achieve the best estimation performance. The optimization problem (6) has been solved using a sequential quadratic programming algorithm (see e.g. [28]), in which the underlying

quadratic programs have been solved with MatLab[®] function `quadprog`. Values of $N \in \{30, 50, 70\}$ (i.e. the number of time steps considered in the MHE problem) have been considered. The corresponding MHEs are denoted as MHE₃₀, MHE₅₀ and MHE₇₀, respectively.

C. DVS design

In order to generate the data needed for the DVS design, the detailed vehicle model described in Section V-A has been simulated in the following maneuvers:

- Random 1. Handwheel angle: uniformly distributed signal filtered to a maximum band of 5 rad/s, taking values in the range $[-63^\circ, 63^\circ]$. Longitudinal speed: uniformly distributed signal filtered to a maximum band of 2.5 rad/s, taking values in the range $[65, 130]$ km/h.
- Steer reversal 30° . Handwheel angle: positive and subsequent negative handwheel angle steps of 30° . Longitudinal speed: 100 km/h constant.
- Steer reversal 60° . Handwheel angle: positive and subsequent negative handwheel angle steps of 60° . Longitudinal speed: 100 km/h constant.
- Steer reversal 80° . Handwheel angle: positive and subsequent negative handwheel angle steps of 80° . Longitudinal speed: 100 km/h constant.
- Test track 1. Steering angle signal and longitudinal speed measured on a real car traveling on a track test. Steering angle: variable in the range $[-50^\circ, 85^\circ]$. Longitudinal speed: variable in the range $[75, 115]$ km/h.

From these maneuvers, a set of 37890 data has been collected with a sampling time of 0.01 s. In order to deal with a not too large set of data, which would lead to a quite long DVS computational time, a subset of data has been selected by taking one sample every ten. The DVS design set, composed of $T = 3789$ data, is thus given by

$$D = \{\tilde{\varphi}_{t-m}^t, \tilde{v}^t, t = 1, 10, \dots, 37890\}.$$

Several DVSs have been designed from this data set by means of the method developed in Section IV. The DVSs are of the form

$$\tilde{v}^t = f_c(\tilde{\varphi}_{t-m}^t)$$

where the function f_c is defined in (19). Regressor orders $m \in \{30, 50, 70\}$ have been considered. For each m , the values of γ and ε required to define f_c have been obtained using the procedure described in [24]. Then, the corresponding DVS has been derived. The designed DVSs are denoted as DVS₃₀, DVS₅₀ and DVS₇₀.

Remark 3: All the data employed in the DVS design have been obtained in the presence of the same road adherence conditions (i.e. dry asphalt). Variable road friction situations can be accounted for, in the context of this study, either by including in the DVS design data collected under different adherence characteristics or, as remarked in [11], through the use of a bank of DVS each one corresponding to a different friction condition.

Estimator	Random 2	Steer reversal 50°	Steer reversal 75°	Steer reversal 85°	Track test 2	Steer step 72° (real data)
MHE ₃₀	0.111	0.284	1988	2720	0.129	3368
MHE ₅₀	0.055	0.130	0.366	2101	0.089	0.744
MHE ₇₀	0.079	0.237	0.450	0.719	0.130	0.654
DVS ₃₀	0.109	0.144	0.123	0.124	0.151	0.508
DVS ₅₀	0.120	0.152	0.135	0.140	0.152	0.420
DVS ₇₀	0.127	0.133	0.242	0.201	0.145	0.453

TABLE I
SIDE-SLIP ANGLE ESTIMATION. RMSE ERRORS (°) PROVIDED BY THE ESTIMATORS ON THE TESTING MANEUVERS.

D. Simulation results

The designed MHEs and DVSs have been tested on four maneuvers not used for estimator design. It should be noted that some of these maneuvers involve large lateral accelerations and thus highly nonlinear lateral dynamics. The maneuvers are the following:

- Random 2. Steering angle: uniformly distributed signal filtered to a maximum band of 5 rad/s, taking values in the range $[-57^\circ, 57^\circ]$ rad. Longitudinal speed: uniformly distributed signal filtered to a maximum band of 2.5 rad/s, taking values in the range [65, 130] km/h.
- Steer reversal 50°: Steering angle: positive and subsequent negative steering angle steps of 50°. Longitudinal speed: 100 km/h constant.
- Steer reversal 75°: Steering angle: positive and subsequent negative steering angle steps of 75°. Longitudinal speed: 100 km/h constant.
- Steer reversal 85°: Steering angle: positive and subsequent negative steering angle steps of 85°. Longitudinal speed: 100 km/h constant.
- Track test 2. Steering angle and longitudinal speed signals measured on a real car during a track test. Steering angle: variable in the range $[-10^\circ, 65^\circ]$. Longitudinal speed: variable in the range [60,100] km/h.

The RMSE (Root Mean Square Error) obtained by the estimators on the testing maneuvers are reported in Table I (columns 2-6). The estimates of DVS₅₀ and MHE₇₀ (the best DVS and the best MHE) are compared to the true signals in Figure 1 for some of the testing maneuvers. From these results, it can be noted that all of the considered estimators provide quite satisfactory estimation accuracies, except for a few maneuvers, where the MHEs show a performance degradation and some unstable behavior. The DVSs are in general more accurate than the MHEs and, thanks to their NFIR structure, cannot be unstable.

Note that the average computational times required for evaluating the estimators at a given time t on a PC with a double 2GHz Xeon processor and 2 GB RAM resulted to be the following: MHE₇₀ computational time = 0.13 s; DVS₇₀ computational time = 0.03 s.

E. Experimental data results

The designed MHEs and DVSs have been tested on an experimental data set, recorded on a real car during the following maneuver:

- Steer step 72°: Steering angle: positive step of 72°. Longitudinal speed: variable in the range [80,110] km/h.

This data set is the same that has been used to validate both the detailed 14 d.o.f. model and the single track model described in Section II.

The RMSE error obtained by the estimators on this real maneuver are reported in Table I (column 7). The estimates of DVS₅₀ and MHE₇₀ are compared to the true signals in Figure 1 (lower-right). It can be noted that all the DVSs provide quite satisfactory accuracies, while the MHEs show larger estimation errors. In order to verify if better results could be obtained by the MHE technique considering a larger horizon, two MHE estimators with orders 120 and 200, respectively, have been tested on the real data maneuver. The RMSE values obtained for these estimators are quite large: 1.621 and 2.2634, respectively.

VI. CONCLUSION

A comparison between a Moving Horizon Estimator (MHE) and a Direct Virtual Sensor (DVS) approach for vehicle side-slip angle estimation has been presented. The MHE filter has been designed on the basis of a simplified nonlinear vehicle model. The DVS has been derived directly from input-output data collected during a preliminary experiment, carried out with a detailed 14 d.o.f. model that simulated the real car. Through extensive simulation tests, it has been shown that the MHE approach can achieve in general quite good accuracy (with some exception), and the DVS approach is able to obtain even better accuracy. The main advantage of the DVS over the MHE approach is that it does not rely on a system model, thus avoiding the issues related to model uncertainty. However, the DVS may need higher memory usage and large data to be collected in an initial experiment, while the MHE can employ a physical system model which may be easy to tune.

REFERENCES

- [1] G. J. Forkenbrock, D. Elsasser, and B. O'Hara, "NHTSA's light vehicle handling and ESC effectiveness research program," *ESV Paper Number 05-0221*, 2005.
- [2] R. Rajamani, *Vehicle Dynamics and Control*. Springer Verlag, 2005.
- [3] G. J. Forkenbrock and P. Boyd, "Light vehicle ESC performance test development," *ESV Paper Number 07-0456*, 2007.
- [4] A. T. V. Zanten, "Bosch ESP systems: 5 years of experience," in *SAE Technical Paper No. 2000-01-1633*, 2000.
- [5] A. von Vietinghoff, M. Hiemer, and U. Kiencke, "Nonlinear observer design for lateral vehicle dynamics," in *16th IFAC World Congress*, Prague, Czech Republic, 2005.
- [6] H. Cherouat, M. Braci, and S. Diop, "Vehicle velocity, side slip angles and yaw rate estimation," in *IEEE ISIE*, Dubrovnik, Croatia, 2005.

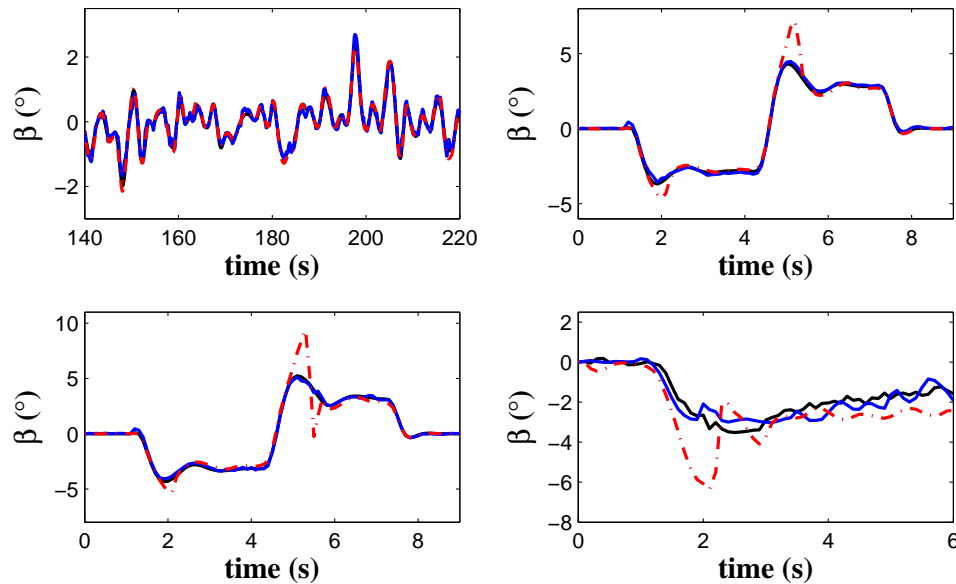


Fig. 1. Side-slip angle estimation. Continuous (black) line: “true” side-slip angle. Dashed (blue) line: DVS₅₀ estimate. Dot-dashed (red) line: MHE₇₀ estimate. Upper-left: Random 2. Upper-right: Steer reversal 75°. Lower-left: Steer reversal 85. Lower-right: Steer step 72° (real data).

- [7] J. Stèphant, A. Charara, and D. Meizel, “Evaluation of sliding mode observer for vehicle sideslip angle,” in *16th IFAC World Congress*, Prague, Czech Republic, 2005.
- [8] H. V. Grip, L. Imsland, T. A. Johansen, T. I. Fossen, J. C. Kalkkuhl, and A. Suissa, “Nonlinear vehicle side-slip estimation with friction adaptation,” *Automatica*, vol. 44, pp. 611–622, 2008.
- [9] S. H. You, J. O. Hahn, and H. Lee, “New adaptive approaches to real-time estimation of vehicle sideslip angle,” *Control Engineering Practice*, vol. 17, pp. 1367–1379, 2009.
- [10] P. Gaspar, Z. Szabo, and J. Bokor, “A grey-box identification of an LPV vehicle model for observer-based side slip angle estimation,” in *American Control Conference*, 2007, pp. 2961–2966.
- [11] V. Cerone, D. Piga, and D. Regruto, “Set-membership LPV model identification of vehicle lateral dynamics,” *Automatica*, vol. 47, pp. 1794–1799, 2011.
- [12] C. Novara, M. Milanese, E. Bitar, and K. Poolla, “The filter design from data (FD2) problem: parametric-statistical approach,” *International Journal of Robust and Nonlinear Control*, vol. 22, pp. 1853–1872, 2012. [Online]. Available: <http://dx.doi.org/10.1002/rnc.1791>
- [13] M. Milanese, D. Regruto, and D. Fortina, “Direct virtual sensors (DVS) design in vehicle sideslip angle estimation,” in *American Control Conference*, 2007, pp. 3654–3658.
- [14] C. Novara, F. Ruiz, and M. Milanese, “Direct identification of optimal sm-lpv filters and application to vehicle yaw rate estimation,” *IEEE Transactions on Control Systems Technology*, vol. 19, no. 1, pp. 5 – 17, jan. 2011.
- [15] —, “Direct filtering: a new approach to optimal filter design for nonlinear systems,” *IEEE Transactions on Automatic Control*, vol. 58, no. 1, pp. 86–99, 2013.
- [16] C. V. Rao, J. B. Rawlings, and D. Q. Mayne, “Constrained state estimation for nonlinear systems: stability and moving horizon approximations,” *IEEE Transactions on Automatic Control*, vol. 48, no. 2, pp. 246–258, 2003.
- [17] A. Alessandri, M. Baglietto, and G. Battistelli, “Moving-horizon state estimation for nonlinear discrete-time systems: New stability results and approximation schemes,” *Automatica*, vol. 44, pp. 1753–1765, 2008.
- [18] H. Zhao and H. Chen, “Estimation of vehicle yaw rate and side slip angle using moving horizon strategy,” in *6th World Congress on Intelligent Control and Automation*, 2006, pp. 1828–1832.
- [19] M. Canale, L. Fagiano, M. Milanese, and P. Borodani, “Robust vehicle yaw control using an active differential and IMC techniques,” *Control Engineering Practice*, vol. 15, pp. 923–941, 2007.
- [20] E. Bakker, L. Lidner, and H. Pacejka, “A new tyre model with an application in vehicle dynamics studies,” in *SAE Paper 890087*, 1989.
- [21] M. Canale and L. Fagiano, “Stability control of 4WS vehicles using robust IMC techniques,” *Vehicle System Dynamics*, vol. 46, no. 11, pp. 911–1011, 2008.
- [22] C. Rao, J. Rawlings, and D. Mayne, “Constrained state estimation for nonlinear discrete-time systems: Stability and moving horizon approximations,” *IEEE Transactions on Automatic Control*, vol. 48, no. 2, pp. 246–258, 2003.
- [23] M. Baes, M. Diehl, and I. Necoara, “Every continuous nonlinear control system can be obtained by parametric convex programming,” *IEEE Transactions on Automatic Control*, vol. 53, pp. 1963–1967, 2008.
- [24] M. Milanese and C. Novara, “Set membership identification of nonlinear systems,” *Automatica*, vol. 40/6, pp. 957–975, 2004.
- [25] M. Canale, C. Novara, and M. Milanese, “NSM constrained approximation of Lipschitz functions from data,” *Systems and Control Letters*, vol. 59, pp. 396–403, 2010.
- [26] C. Novara, F. Ruiz, and M. Milanese, “A new approach to optimal filter design for nonlinear systems,” in *48th IEEE Conference on Decision and Control and European Control Conference*, Shanghai, China, 2009.
- [27] M. Milanese and C. Novara, “Computation of local radius of information in SM-IBC identification of nonlinear systems,” *Journal of Complexity*, vol. 23, p. 937–951, 2007.
- [28] J. Nocedal and S. Wright, *Numerical Optimization*. New York: Springer, 2006.